*Article*

# Asymmetrical cross-sectional buckling in arc-prepared multi-wall carbon nanotubes revealed by iodine filling

**Abraao Cefas Torres-Dias[1], Anthony Impellizzeri[2], Emmanuel Picheau[3], Laure Noé[1], Alain Pénicaud[3], Christopher Ewels[2*] and Marc Monthioux[1*]**

[1] Centre d'Elaboration des Matériaux et d'Etudes Structurales (CEMES), CNRS, Université de Toulouse, 31055 Toulouse, CEDEX 04, France
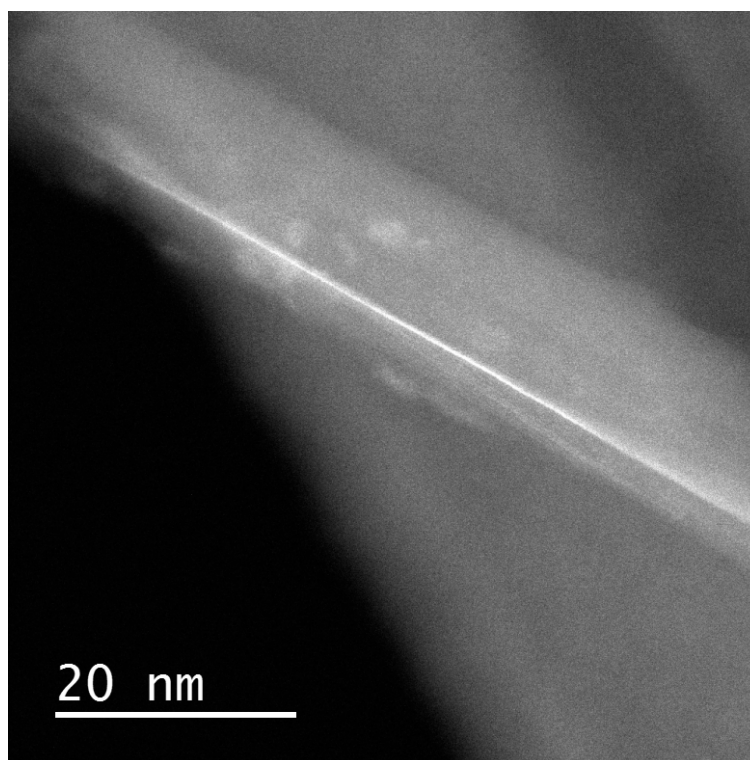[2] Institut des Matériaux Jean Rouxel, CNRS, Université de Nantes, 44000 Nantes, France
[3] Centre de Recherche Paul Pascal (CRPP), CNRS, Université de Bordeaux, 33600 Pessac, France
[*] Correspondence: authors: marc.monthioux@cemes.fr (M. Monthioux); chris.ewels@cnrs-imn.fr (C. Ewels)

### Additional High Angle Annular Dark Field (HAADF) STEM images

HAADF is sensitive to atomic number and therefore provides high contrast between carbon and iodine atoms. With this imaging technique, the presence of iodine in carbon nanotubes (CNTs) is thus revealed by a brighter contrast. **Figure S1** shows iodine forming a linear configuration (that we call iodine line for simplicity) in-between the shells of a multi-walled CNT (MWCNT).

**Figure S1.** Lower magnification HAADF image corresponding to the bright-field image shown in **Figure.5a** of the main text.

**Figure S2** reveals several (though weaker) iodine lines which are difficult to count. At least one of these lines is not parallel to the axis of the nanotube. As this image is a projection of a tubular structure seen longitudinally, we propose that this line has a helical geometry. As shown in the main text, the channels in which iodine atoms are inserted can be either straight and parallel (as in **Figure.3**) or helical (as in **Figure.4**) with respect to the CNT elongation axis. **Figure S2** suggests that both can be present in the same CNT. As

the helical character of the channels was speculated to be chirality-induced, **Figure S2** could thus result from a chirality change among the MWCNT shells.
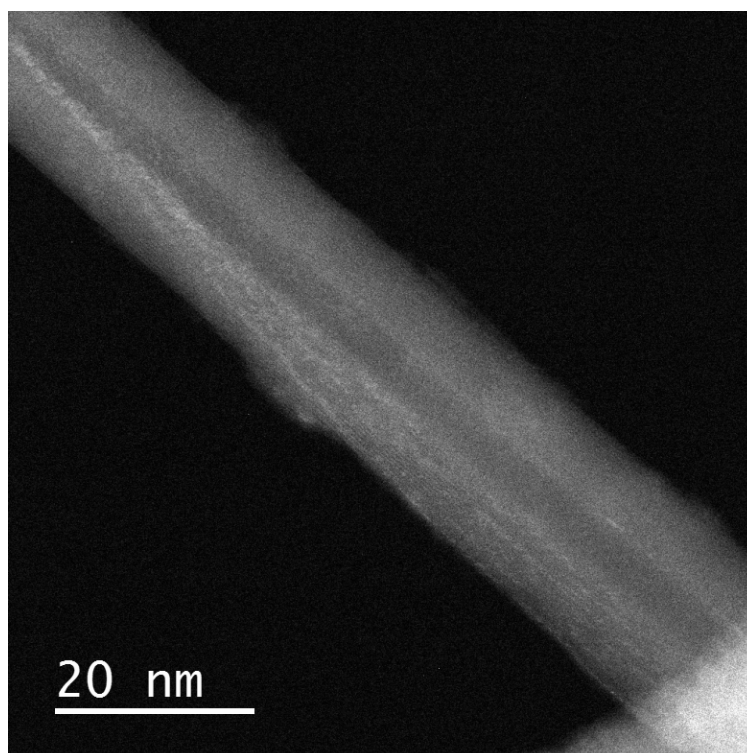


**Figure S2.** Lower magnification HAADF image corresponding to the bright-field image shown in **Figure.5c** of the main text.

## Geometry of Zig-zag DWCNTs

**Table S1.** DFT-D2 optimized geometry parameters of zig-zag DWCNT (n,0)@(n+x,0) combinations, where x = 8, 9, and 10. The intershell spacing d of the unrelaxed case when both shells have the same central axis are indicated in brackets beneath the tube description. The minimum ($d_{min}$) and maximum ($d_{Max}$) intershell distance, and the difference between them ($\Delta d$) are given in nm. This table includes all values represented in Figure 10 shown in the main text.

| Tube combination ($d_{unrelaxed}$) | Helicity index | $d_{min}$ (nm) | $d_{max}$ (nm) | $\Delta d$ (nm) |
|---|---|---|---|---|
| (n,0)@(n+8,0) (0.313 nm) | (13,0)@(21,0) | 0.319 | 0.319 | 0.000 |
| | (19,0)@(27,0) | 0.323 | 0.323 | 0.000 |
| | (25,0)@(33,0) | 0.326 | 0.326 | 0.000 |
| | (31,0)@(39,0) | 0.329 | 0.329 | 0.000 |
| | (37,0)@(45,0) | 0.332 | 0.332 | 0.000 |
| | (43,0)@(51,0) | 0.327 | 0.333 | 0.006 |
| | (49,0)@(57,0) | 0.323 | 0.335 | 0.013 |
| | (61,0)@(69,0) | 0.325 | 0.336 | 0.011 |
| (n,0)@(n+9,0) (0.344 nm) | (13,0)@(22,0) | 0.349 | 0.355 | 0.006 |
| | (19,0)@(28,0) | 0.347 | 0.352 | 0.005 |
| | (25,0)@(34,0) | 0.345 | 0.347 | 0.002 |
| | (31,0)@(40,0) | 0.345 | 0.346 | 0.001 |
| | (37,0)@(46,0) | 0.343 | 0.346 | 0.003 |
| | (43,0)@(52,0) | 0.337 | 0.347 | 0.010 |
| | (49,0)@(58,0) | 0.336 | 0.346 | 0.010 |

| | | | | |
|---|---|---|---|---|
| | (61,0)@(70,0) | 0.336 | 0.347 | 0.011 |
| | (13,0)@(23,0) | 0.343 | 0.568 | 0.225 |
| | (19,0)@(29,0) | 0.340 | 0.598 | 0.258 |
| | (25,0)@(35,0) | 0.342 | 0.618 | 0.276 |
| | (31,0)@(41,0) | 0.346 | 0.617 | 0.271 |
| (n,0)@(n+10,0) (0.376 nm) | (37,0)@(47,0) | 0.347 | 0.612 | 0.265 |
| | (43,0)@(53,0) | 0.346 | 0.625 | 0.279 |
| | (49,0)@(59,0) | 0.346 | 0.628 | 0.282 |
| | (61,0)@(71,0) | 0.345 | 0.625 | 0.280 |

**Iodine Bilayer Graphene Intercalation Compounds**

Zig-zag DWCNTs have carbon atoms in a zig-zag [$2\bar{1}\bar{1}0$] orientation around the circumference. If now projected to resemble bilayer graphene (2LG), the tangential shear along the [$2\bar{1}\bar{1}0$] direction makes the interlayer stacking type of the bilayer vary. We investigated the iodine intercalation and adsorption in 2LG with varying translational shearing along [$2\bar{1}\bar{1}0$] between the two layers. Two stacking orders are here considered: AA and AA'. In the AA-stacking sequence, every carbon atom of one layer is exactly superimposed to the carbon atom of the next one. In the AA′-stacking order, the C-C dimer of the hexagon of one layer is placed in the middle of the hexagon of the second layer [41–43], as illustrated in **Figure S3**.
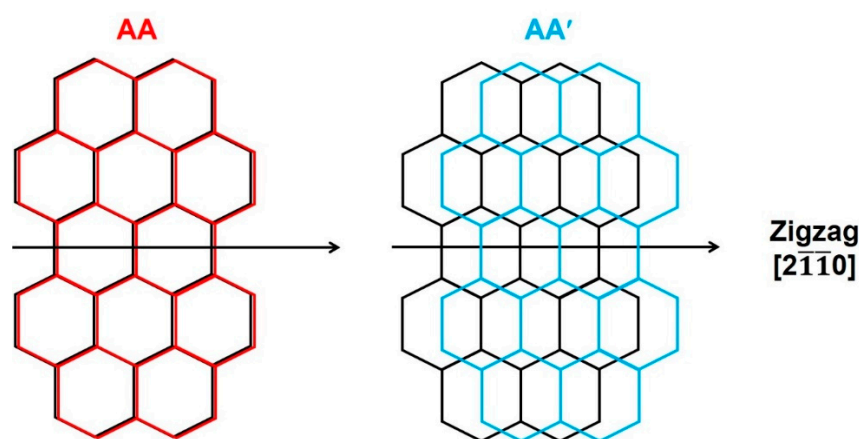


**Figure S3.** Schematic representation of the displacement along the zig-zag direction (horizontal black arrow) of the lattice structures of two superimposed graphenes forming a 2LG. The lattice of the lower fixed layer is represented in black, while that of the moving upper one is represented in red and blue for the AA and AA′ stacking systems, respectively. .

Both the atomic positions and in-plane lattice vectors of an orthorhombic unit cell of bilayer graphene are fully optimized with $16 \times 16 \times 1$ k-point mesh grid. After forming the supercell, we added iodine either between the graphene layers or above the carbon surface (both are tested). The resultant configurations were re-optimized with a $2 \times 4 \times 1$ k-point mesh grid. Periodicity along the cell axis means the iodine forms lines with iodine atom spacing of 0.426 nm.

Figure S4 shows the total energy difference between iodine either intercalated or adsorbed in 2LG by increasing the width of graphene layers. The intercalation of iodine between graphene layers is metastable with respect to iodine adsorption. This is because the small initial interlayer spacing requires large distortion of the graphenes in order to incorporate the iodine, which carries a significant energy penalty both in terms of bonding distortion and reduction of interlayer van der Waals interactions. This is a main difference

with MWCNTs having large nanochannel-like spacing between carbon shells, where iodine is stabilised in the buckled side.
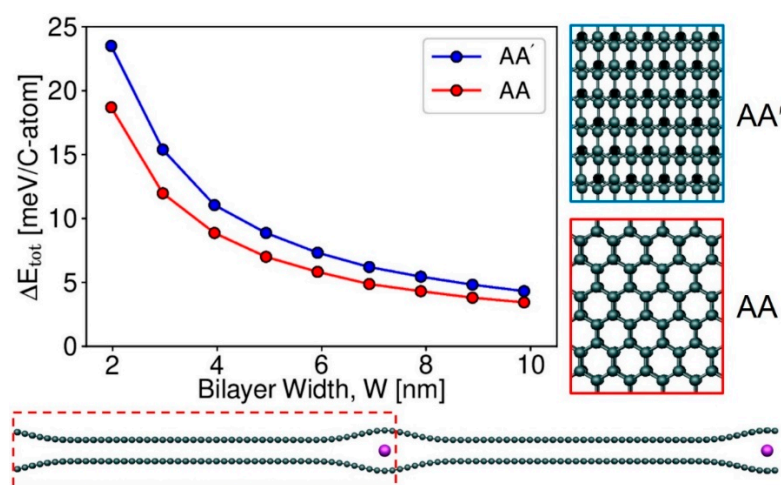


**Figure S4.** DFT-D2 computed total energy difference between iodine either intercalated or adsorbed for (red) AB'- and (blue) AA-stacked 2LG as a function of the layer width. Below is provided a model of the bilayer graphene showing the formation of the buckled bulb after iodine intercalation that has been relaxed. Dashed red rectangle represents the conventional unit cell (6.171 nm in this case).

It is widely accepted that AA′-stacked bilayer is energetically favoured compared to AA-stacked configuration. However, interestingly, iodine intercalation changes this hierarchy, making the AA-stacking the lowest energy one [44,45].

### Helicity-Dependent Intercalation of Iodine Chains into DWCNTs

We tested two sets of DWCNTs with armchair helicity: $(n,n)@(n+5,n+5)$ and $(n,n)@(n+6,n+6)$. While the $(n,n)@(n+5,n+5)$ shell pairing is characterised by an intershell distance equal to 0.339 nm, the $(n,n)@(n+6,n+6)$ combination shows an intershell spacing of 0.392 nm. The radially uniform geometry of the $(n,n)@(n+5,n+5)$ tube pair is totally independent from the distance variation between the shells. Given the larger intershell spacing, the $(n,n)@(n+6,n+6)$ tube pair is subjected to the out-of-plane deformation by varying the interlayer distance. The lowest-energy configuration for the armchair $(n,n)@(n+6,n+6)$ combination is characterised by the appearance of one buckled side, like its zig-zag counterpart. The resulting optimised geometry parameters are reported in **Table S2**.

**Table S2.** DFT-D2 optimised geometry parameters of armchair DWCNT (n,n)@(n+x,n+x) combinations, where x = 5 and 6. The diameter of the outer shell (in nm) is provided, as well the minimum ($d_{min}$) and the maximum ($d_{max}$) intershell distance between the un-buckled and the buckled sides, respectively. $\Delta d$ is the difference between these two values. Bracketed numbers in the left column indicate the intershell spacing for the initial unrelaxed axially symmetric cylindrical tubes.

| Tube Combination ($d_{unrelaxed}$) | Helical index | Outer diameter (nm) | $d_{min}$ (nm) | $d_{max}$ (nm) | $\Delta d$ (nm) |
|---|---|---|---|---|---|
| | (8,8)@(13,13) | 1.778 | 0.341 | 0.345 | 0.004 |
| | (14,14)@(19,19) | 2.592 | 0.344 | 0.351 | 0.007 |
| (n,n)@(n+5,n+5) | (20,20)@(25,25) | 3.408 | 0.345 | 0.350 | 0.005 |
| (0.339 nm) | (26,26)@(31,31) | 4.225 | 0.348 | 0.350 | 0.002 |
| | (32,32)@(37,37) | 5.042 | 0.348 | 0.351 | 0.003 |
| | (8,8)@(14,14) | 1.909 | 0.346 | 0.638 | 0.292 |
| | (14,14)@(20,20) | 2.725 | 0.343 | 0.705 | 0.362 |
| (n,n)@(n+6,n+6) | (20,20)@(26,26) | 3.542 | 0.345 | 0.762 | 0.417 |
| (0.392 nm) | (26,26)@(32,32) | 4.359 | 0.346 | 0.776 | 0.430 |

| | | | |
|---|---|---|---|
| (32,32)@(38,38) | 5.175 | 0.356 | 0.700 | 0.344 |

The following table (**Table S3**) shows the energy difference between chains of iodine atoms inserted either between the two graphene shells of the DWCNTs described above, or placed inside the central cavity next to the internal graphene shell. Negative values indicate that the iodine is more stable intercalated between the two carbon shells. This table shows that the intra-shell intercalation behaviour shown in the main paper is independent of shell chirality.

**Table S3.** Calculated DFT-PBE+D2 energy difference (meV/C-atom) between an linear iodine chain inside the internal shell and the same intercalated between the carbon shells for various zig-zag and armchair DWCNTs. A negative energy difference indicates the iodine is more stable when intercalated between the carbon shells. .

| Helicity | Helical index | Outer Diameter (nm) | ΔE (meV/C-atom) |
|---|---|---|---|
| Zig-zag | (13,0)@(23,0) | 1.812 | +0.85 |
| | (25,0)@(35,0) | 2.754 | -1.28 |
| | (37,0)@(47,0) | 3.696 | -1.09 |
| | (49,0)@(59,0) | 4.639 | -0.90 |
| Armchair | (8,8)@(14,14) | 1.909 | +0.01 |
| | (14,14)@(20,20) | 2.725 | -1.40 |
| | (20,20)@(26,26) | 3.542 | -1.17 |
| | (26,26)@(32,32) | 4.359 | -1.08 |

**Tri-Iodide Intercalation in DWCNTs**

**Figure S5.** shows the relative stability between tri-iodide inside and intercalated in a zig-zag (25,0)@(35,0) DWCNT. The optimised I-I bond length of the trimer confined inside the internal shell and the buckle is 0.296 and 0.297 nm, respectively. The bond angle associated to the trimer is 178.6° and 179.7° for the two configuration of interest, respectively. The comparison of the relative energies in this case shows that the iodine intercalation between the carbon shells is energetically favored by 0.720 meV/C-atom. The resulting sum of Mulliken charges for the tri-iodide molecule is -1.028 corresponding to a classic stable $I_3^-$ ion, and that the value for iodine encapsulated inside the internal tube is higher than -0.867.
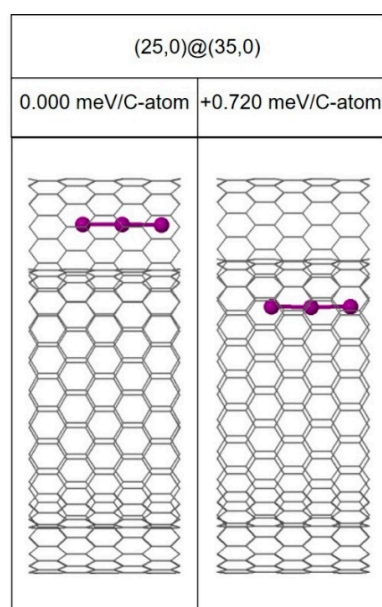


**Figure S5.** Side view of DFT-D2 relaxed super-cell of tri-iodide-filled (25,0)@(35,0) zig-zag DWCNT. Two positions for the iodine trimer were tested: (left) intercalated between the graphene

shells, and (right) inside the internal shell. The intercalated structure on the left is more stable, by +0.720 meV per carbon atom (+172.933 meV per iodine atom).

### Iodine Intercalation in MWCNTs

*Triple-walled case:* We next extented the investigation to triple-walled carbon nanotubes (TWCNTs) considering the following two combinations: (25,0)@(33,0)@(43,0) and (25,0)@(35,0)@(43,0), as shown in **Figure S5**, again with a linear iodine chain spaced by 0.426 nm. In both cases, we observe the formation of local buckling when the helical index difference is $\Delta n = 10$. As for DWCNTs, iodine intercalation inside the buckled side is energetically favored with respect to iodine placed inside the innermost tube. Intershell intercalation again allows higher carbon-iodine interaction and higher charge transfer (+0.090$e$) with respect to iodine within the internal tube cavity.
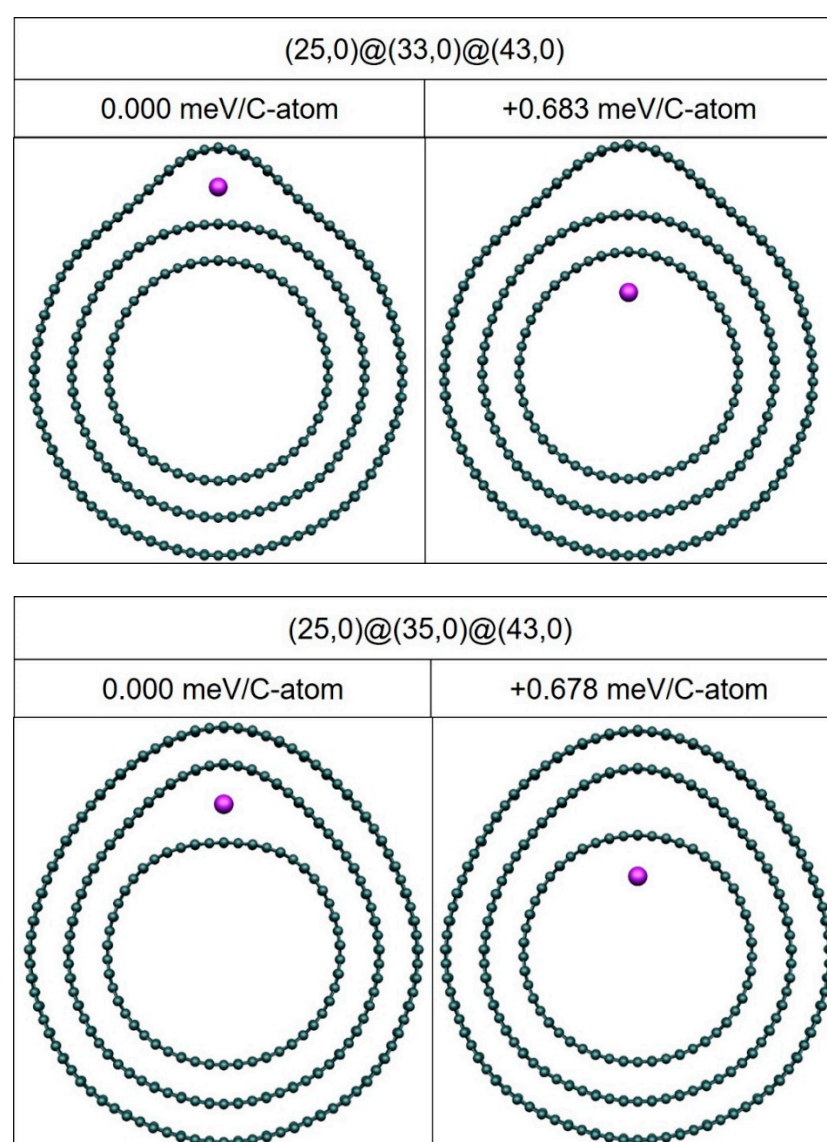


**Figure S6.** Optimised structure of iodine-filled **(top)** (25,0)@(33,0)@(43,0) and **(bottom)** (25,0)@(35,0)@(43,0) zig-zag TWCNTs. Two positions for the iodine line were tested: **(left)** intercalated between shells with the helical index difference set to 10; **(right)** inside the innermost shell. All energy values (in meV/C-atom) are given with respect to the most stable configurations shown on the left.

**Figure S7** shows the optimised geometry of two iodine-filled zig-zag TWCNTs (*37,0)@(45,0)@(55,0)* and *(37,0)@(47,0)@(55,0)*, where the helical index difference between the constituting shells is 8 and 10 for the first combination and vice-versa for the second one. The iodine intercalation is energetically favored between the shells of a DWCNT characterised by a helical index difference of 10. This further confirms that both buckling and iodine filling behaviour is purely a function of the intershell spacing and is independent of either the number of shells, as highlightd in **Figure S8**.
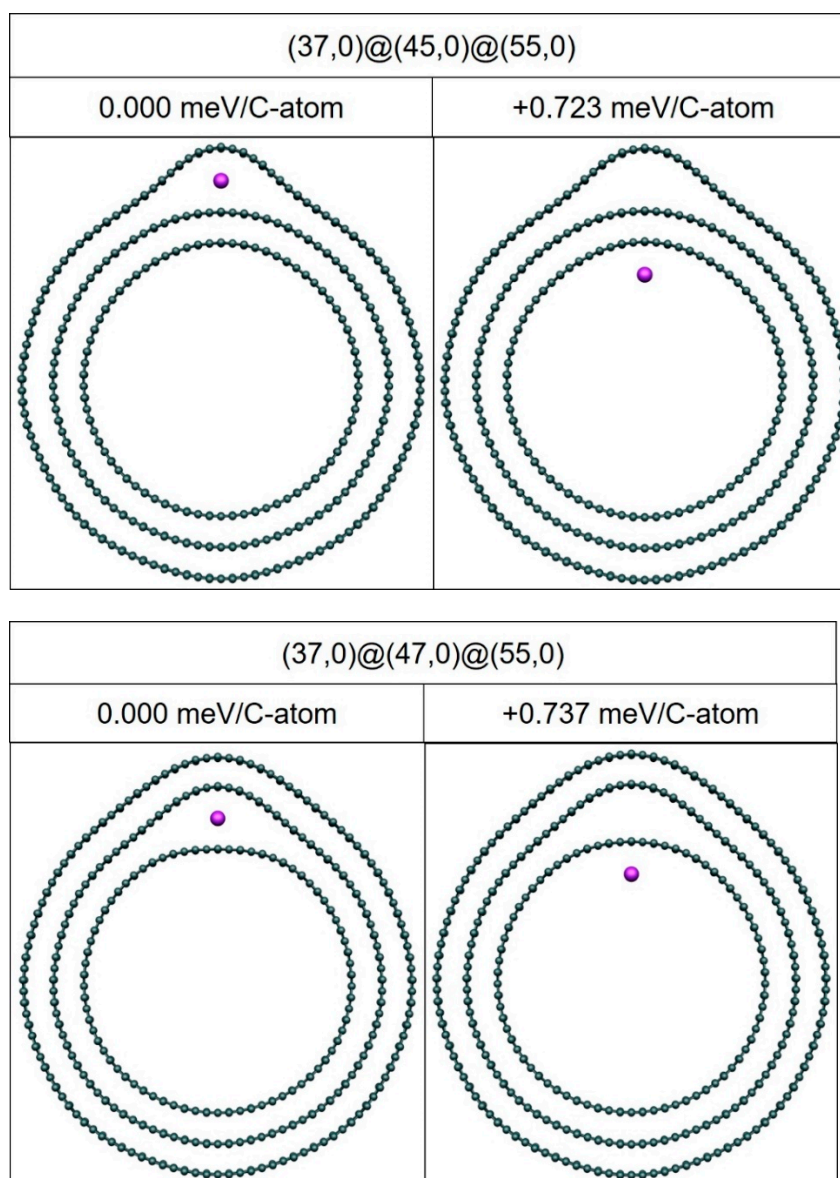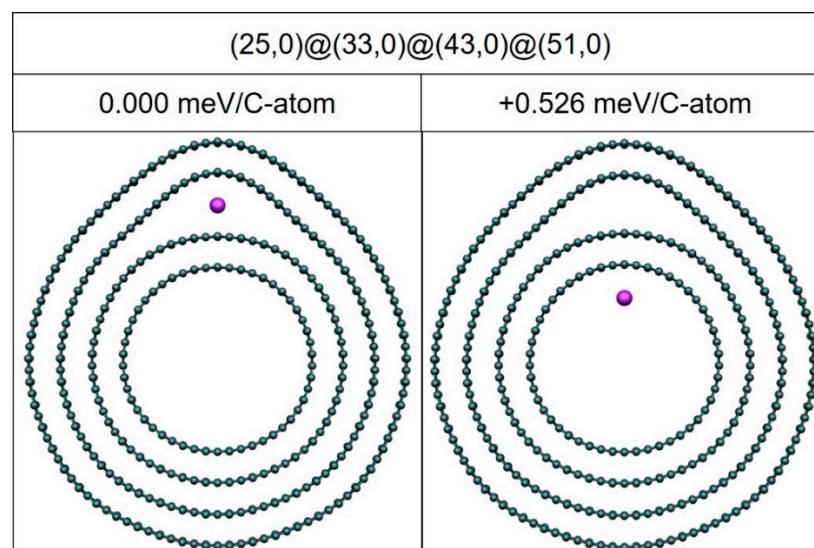


**Figure S7.** Optimised structure of iodine-filled **(top)** (37,0)@(45,0)@(55,0) and **(bottom)** (37,0)@(47,0)@(55,0) zig-zag TWCNTs. Two positions for the iodine line were tested: **(left)** intercalated between shells with the helical index difference set to 10, **(right)** inside the innermost shell. All energy values (in meV/C-atom) are given with respect to the most stable configurations placed on the left.
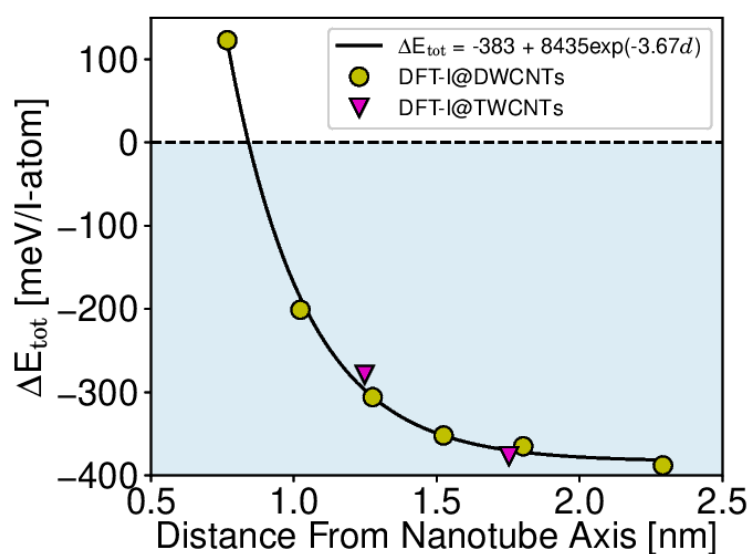
**Figure S8.** DFT-D2 calculated total energy difference per iodine atom of (green circles) DWCNTs and (magenta triangles) TWCNTs versus the separation distance between iodine atom and nanotube axis. The solid black curve shows the exponential fitting equation: $\Delta E_{tot}$ (meV/I-atom)= -383 + 8435exp(-3.67d), where d represents the separation distance between the iodine line and the nanotube centre.

*Quadri-walled case:* the same analysis was performed on a *(25,0)@(33,0)@(43,0)@(51,0)* quadri-walled carbon nanotube (QWCNT), where the helical index difference between the second and third shells is set to 10. Once optimised, the resulting cross-section exhibits the formation of a buckled side. As above we next filled the deformed region with an iodine chain and calculated the relative energy per carbon atom (**Figure S9**). Like in the DWCNT and TWCNT cases, the iodine is more stabilised within the buckled bulge rather than inside the smallest-diameter shell.



**Figure S9.** Optimised structure of iodine-filled (25,0)@(33,0)@(43,0)@(51,0) zig-zag QWCNT. Two positions for iodine line were tested: **(left)** intercalated between shells with the helical index difference set to 10, **(right)** inside the innermost shell. All energy values (in meV/C-atom) are given with respect to the most stable configuration shown on the left.

Although the number of simulated carbon shells is significantly lower than in the actual MWCNTs experimentally observed, we have fully demonstrated that iodine chain stability is largely independent of the number of the graphene shells.

## References

41. Lee, J.-K.; Lee, S.-C.; Ahn, J.-P.; Kim, S.-C.; Wilson, J.I.B.; John, P. The Growth of AA Graphite on (111) Diamond. *J. Chem. Phys.* **2008**, *129*, 234709. https://doi.org/10.1063/1.2975333.
42. Lee, J.-K.; Lee, S.; Kim, Y.-I.; Kim, J.-G.; Lee, K.-I.; Ahn, J.-P.; Min, B.-K.; Yu, C.-J.; Hwa Chae, K.; John, P. Structure of Multi-Wall Carbon Nanotubes: AA′ Stacked Graphene Helices. *Appl. Phys. Lett.* **2013**, *102*, 161911. https://doi.org/10.1063/1.4802881.
43. Lee, J.-K.; Kim, J.-G.; Hembram, K.P.S.S.; Kim, Y.-I.; Min, B.-K.; Park, Y.; Lee, J.-K.; Moon, D.J.; Lee, W.; Lee, S.-G.; et al. The Nature of Metastable AA′ Graphite: Low Dimensional Nano- and Single-Crystalline Forms. *Sci. Rep.* **2016**, *6*, 39624. https://doi.org/10.1038/srep39624.
44. Yaya, A.; Ewels, C.P.; Suarez-Martinez, I.; Wagner, P.; Lefrant, S.; Okotrub, A.; Bulusheva, L.; Briddon, P.R. Bromination of Graphene and Graphite. *Phys. Rev. B* **2011**, *83*, 045411.
45. Hof, F.; Impellizzeri, A.; Picheau, E.; Che, X.; Pénicaud, A.; Ewels, C.P. Chainlike Structure Formed in Iodine Monochloride Graphite Intercalation Compounds. *J. Phys. Chem. C* **2021**, *125*, 23383–23389.